Applied Surface Science 594 (2022) 153364

Contents lists available at ScienceDirect

Applied Surface Science

journal homepage: www.elsevier.com/locate/apsusc

Full length article

Low coverage disordered decanethiol monolayers on Au(001): A conjecture regarding the formation of Au-adatom-molecule complexes

Martina Tsvetanova [a,*], Alexey G. Syromyatnikov [b], Harold J.W. Zandvliet [a], Andrey L. Klavsyuk [b], Kai Sotthewes [a]

[a] Physics of Interfaces and Nanomaterials, MESA+ Institute for Nanotechnology, University of Twente, Post Office Box 217, Enschede, 7500AE, Netherlands
[b] Faculty of Physics, Lomonosov Moscow State University, Moscow, 119991, Russian Federation

ARTICLE INFO

MSC:
0000
1111

Keywords:
STM
Decanethiol
Au-adatom
Au(001)
DFT
Diffusion

ABSTRACT

We present a scanning tunneling microscopy study of decanethiol on Au(001) in the low coverage regime. As expected, the hex reconstruction is lifted, however, no ordered decanethiol phases form. We observe large areas free of Au islands and covered with a disordered decanethiol phase. $I(t)$ spectroscopy measurements suggest that this disordered phase is dynamic and most likely comprises diffusing Au adatoms, decanethiol molecules, and/or Au-adatom-decanethiol molecule complexes. We have performed density functional theory calculations and show that the activation barrier for diffusion is lower when Au-adatom-molecule complexes are considered in comparison to the case of bare molecule. These findings suggest that although no vacancy pits form on Au(001), Au-adatoms expelled during the lifting of the hex reconstruction may be still important for the diffusion of thiol molecules on this surface.

1. Introduction

The (001) surface of Au reconstructs into the so-called hex phase: an anisotropic hexagonally distorted pattern of ~25% higher atom density compared to the underlying (1 × 1) lattice [1,2]. The hex reconstruction has a complex unit cell, variations of which exist depending on the preparation [3]. The unit cell is generally given by $(5 \times N)$, where $N \sim 20$ [4]. This complex reconstruction has been extensively studied in real and reciprocal space, as well as in theoretical studies [1–16], and can be easily manipulated in electrochemical environment, where a controlled reversible transition between Au(001)-(1 × 1) and Au(001)-hex has been established [17–24]. It was shown that the hex reconstruction is sensitive to surface charging. When charge is accumulated at the Au surface due to an applied electrode potential, the hex reconstruction is lifted, a process that is most likely also sensitive to specific anion adsorption [24–26].

The formation of thiol monolayers on Au(001) was also shown to be accompanied by the lifting of the hex phase, even without electrode potential control [27–32] and also in UHV conditions [33], a process similar to the lifting of the herringbone reconstruction in the case of thiol self-assembled monolayers (SAMs) on Au(111) [34,35]. However, the thiol SAM formation mechanisms have been treated differently in scientific reports concerning these surfaces, which is related to a key difference between Au(111) and Au(001). In the case of Au(111), the thiol SAM formation proceeds along with the appearance of vacancy pits [36] on the surface terraces, absent in the case of thiol monolayers on Au(001).

It is widely accepted that the vacancy pits in the case of thiol SAMs on Au(111) originate from thiol molecules forming a staple, i.e. a molecule-Au-adatom complex (usually of the form RS–Au–SR), which emerges after the deprotonation of thiol molecules and which can diffuse on the surface as the basic building block of the SAM [37–39]. The staple is generally excluded as a building block of thiol phases on Au(001) as for this surface it was shown that the bridging configuration (–RS–) is preferred over the staple motif [40]. A very comforting argument in favor is given by a study of hexanethiol directly adsorbed on the Au(001)-(1 × 1) surface [31], which cannot supply $\theta \sim 0.25$ of Au-adatoms, as the hex reconstruction is already lifted. The adsorption of hexanethiol still does not lead to the formation of vacancy islands, which would be required if staples were indeed the leading moieties. For some ringed thiols like 6-Mercaptopurine, the adsorption on Au(001)-hex also does not show evidence of the staple as a building block of the SAM [41], although Au-adatom rows are part of some of the phase models reported. This molecule also does not form staples on Au(111), nor on Au(001)-(1 × 1) [42,43]. However, after its desorption from the Au(111) surface, small Au islands form. Therefore, in all cases,

* Corresponding author.
E-mail addresses: m.tsvetanova@utwente.nl (M. Tsvetanova), k.sotthewes@utwente.nl (K. Sotthewes).

https://doi.org/10.1016/j.apsusc.2022.153364
Received 14 December 2021; Received in revised form 24 March 2022; Accepted 8 April 2022
Available online 22 April 2022

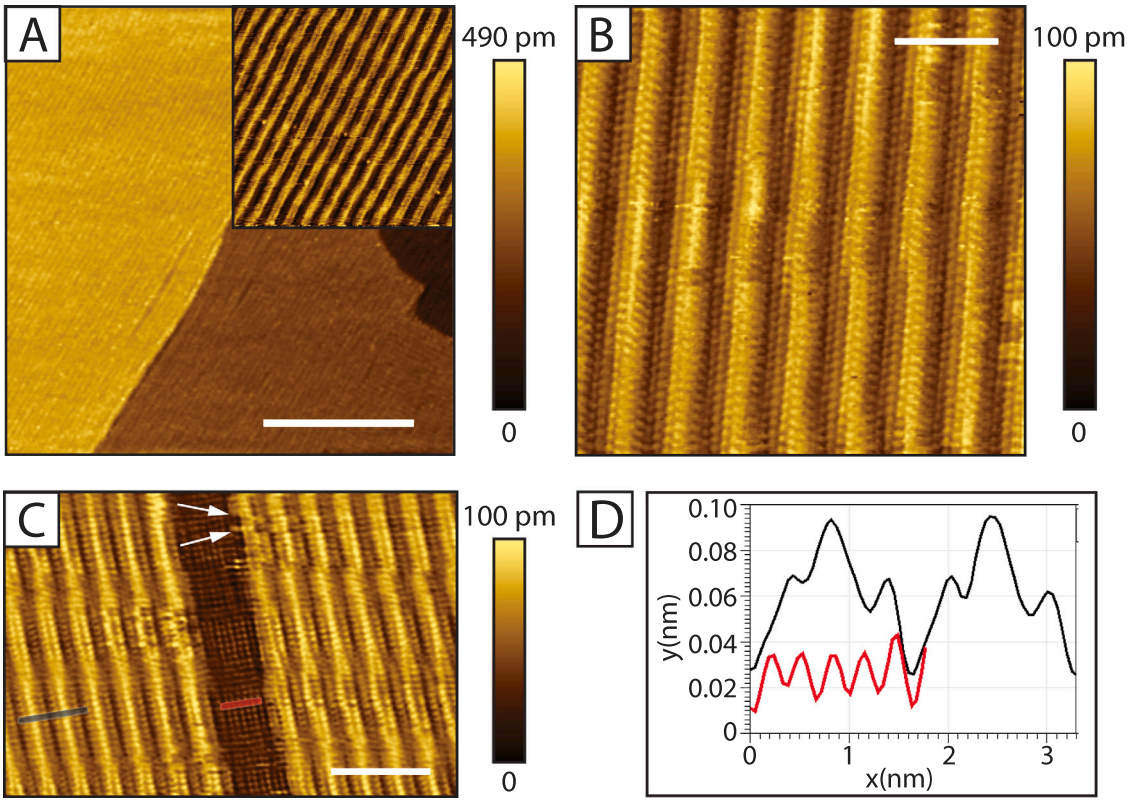

Fig. 1. STM data from the Au(001) surface. (A) The Au(001) surface featuring the hex reconstruction, closely aligned with the substrate steps, set-points: −200 mV, −0.6 nA, scale bar: 40 nm, inset: 22 × 22 nm^2. (B) A zoomed-in image of the hex reconstruction, set-points: −90 mV, −500 pA, scale bar: 3 nm. (C) The hex reconstruction next to a small Au(001)-(1 × 1) region, set-points: −300 mV, −400 pA, scale bar: 5 nm. The profile lines are color-coded and correspond to the height profiles in (D). The hex overlayer features a slight rotation (<1°) w.r.t. the bulk-truncated surface. Arrows point to some of the first lateral switching effects taking place perpendicular to the hex rows. (D) Height profiles corresponding to the analogously colored lines in (C), showing that the width of the hex overlayer corresponds to 5 Au lattice spacings of the unreconstructed surface.

even though the staple is not a majority motif on the surface, the role of molecule-Au-adatom complexes cannot be ruled-out.

Based on our discussion so far, there is no general reason to exclude the Au-adatom-molecule complex as a diffusing entity on Au(001). Grumelli et al. [30] have shown that in the case of hexanethiol it may be possible that Au-adatom-molecule complexes participate in anisotropic diffusion process, which allows the formation of elongated Au islands, decorated with a hexanethiol phase. They have also observed serrated step edges in the vicinity of these islands. Moreover, for S adlayers on Au(001) it was reported that sulfur dimers form S–Au complexes with Au-adatoms [44].

Although, the basic building blocks of thiol phases on Au(001) may not be the staples, we suggest that molecule-Au-adatom structures may be still important for the transport of molecules. In this paper, we present results concerning a low coverage regime, for which no ordered decanethiol phases form. Based on topographic and spectroscopic measurements, we suggest the universal conjecture that irrespective of the surface orientation, molecule-Au-adatom structures may always be important diffusing entities on gold surfaces, even if not the majority moieties.

2. Methods

In this research, a Au(001) single crystal is used as a substrate (purchased by SPL, Zaandam, the Netherlands). The surface was cleaned by several Ar^+ sputtering cycles with ion energy of 1 keV and a time period per cycle between 20 and 45 min. The base pressure in the UHV system was $<1 \cdot 10^{-9}$ mbar, while the Ar pressure was $\sim 3 \cdot 10^{-6}$ mbar. After each sputtering cycle, the sample was annealed ex-situ in a quartz tube oven for 12 h at a temperature of 600 °C under a constant N_2 flow. After a few cycles were performed, the Au(001) surface featured the expected hex reconstruction, measured with an RHK Technology scanning tunneling microscope (STM) at room temperature. The STM tips were electrochemically etched from a Pt-Ir wire. The SAM was prepared via the solution-based method. The Au(001) single crystal was submerged in a 1 mM 1-decanethiol (99% purity, purchased by Sigma Aldrich) ethanolic solution for 1 h. Afterwards, the sample was rinsed with copious amount of ultrapure ethanol and dried with N_2. The freshly prepared sample was loaded in UHV conditions as soon as possible to avoid prolonged exposure to air and potential contamination. During an STM measurement, the tip is biased, and the sample is grounded.

3. Computational details

The *ab initio* density functional theory (DFT) calculations of the activation barriers for diffusion were performed using the Vienna *ab initio* simulation package (VASP) [45,46]. The ion–electron interaction was described using the projector augmented-wave (PAW) technique [47,48]. We used the GGA-PBE density functional [49]. It has been demonstrated that the PBE-GGA functional achieves a good balance between accuracy and computational effort for the gold–decanethiol system [50]. We used a plane-wave basis set with a kinetic energy cut-off of 400 eV. The substrate was modeled as periodically repeated slabs, consisting of up to five atomic layers, separated by a sufficiently thick vacuum layer. The bottom two layers of the slab were fixed at their bulk positions. The top three layers were allowed to relax upon optimization. The atomic positions were relaxed until the force on the unconstrained atoms was less than 0.03 eV Å^{-1}. In all our calculations we have used a (4 × 8 × 1) Monkhorst–Pack **k**-point grid [51] to sample the Brillouin zone of the surface unit cell. The contributions of van der Waals forces were estimated by using dDsC

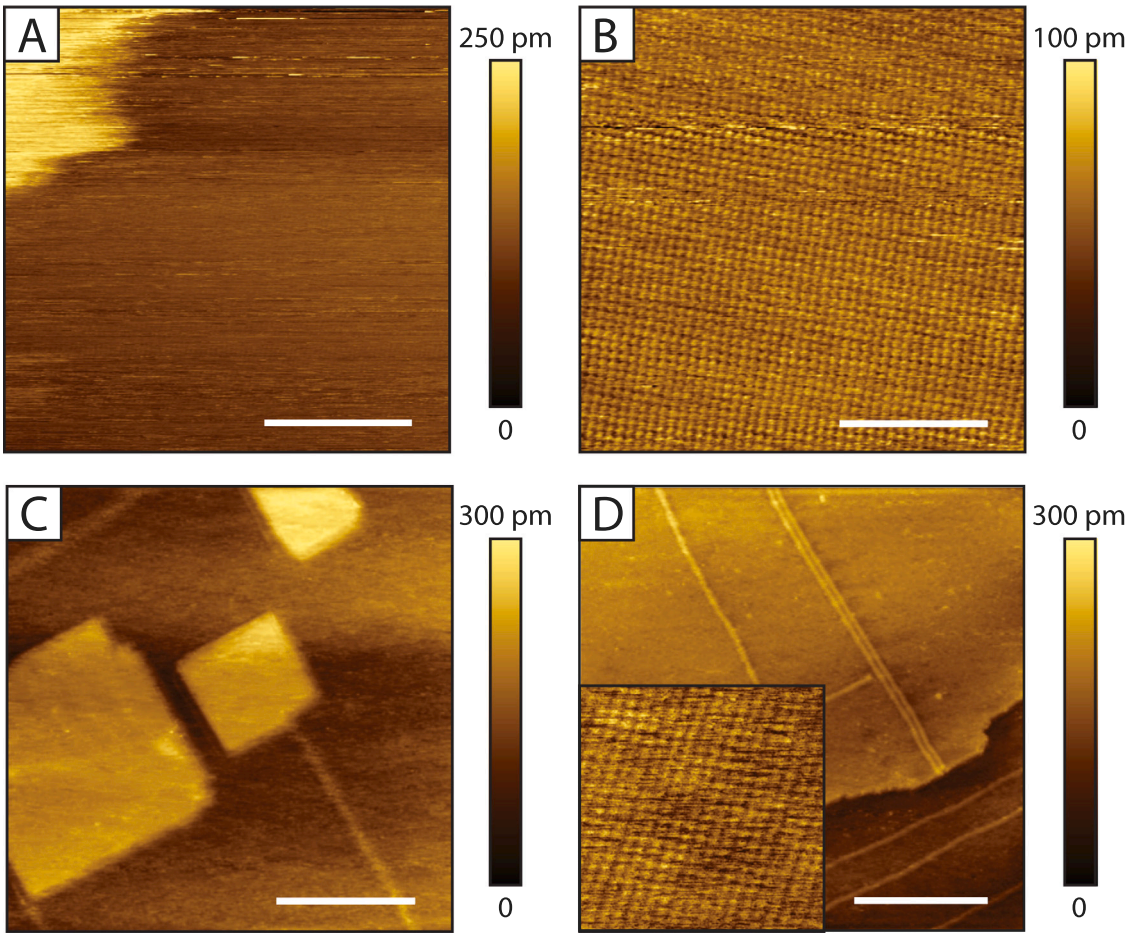

Fig. 2. STM data from the decanethiol-modified Au(001) surface. (A) Local molecular landscape. Because of a lot of interaction with the tip, the step at the top left corner appears distorted, probably due to dynamics at the step-edge. The remaining areas feature disordered phase. Set-points: 500 mV, 80 pA, scale bar: 10 nm. (B) A zoomed-in image from a flat area near the region in (A), showing the Au(001)-(1 × 1) lattice. Set-points: 500 mV, 80 pA, bar: 5 nm. (C) Another local molecular landscape, featuring a few islands and occasionally a few hex stripes as shown in (D). Set-points: 500 mV, 80 pA, scale bar: 25 nm. (D) Set-points: 300 mV, 100 pA, scale bar: 30 nm, inset: 6 × 6 nm^2. The inset shows the lattice between the hex stripes, corresponding to the Au(001)-(1 × 1) lattice (upon increasing the current set-point to 300 pA). The scan angle was changed, the Au(001)-(1 × 1) lattice is actually aligned with the hex stripes.

dispersion corrections [52]. To study the diffusion of a molecule on the gold surface, we employed the nudged elastic band method [53,54] implemented in VASP to locate the saddle points of the potential energy surface and search for the minimum energy pathway of diffusion. The minimum energy path was discretized by nine intermediate states between two states. The atomic models were created using VESTA [55].

4. The Au(001) surface landscape

Before putting the Au(001) single crystal in the decanethiol solution, the surface features the hex reconstruction, as shown in Fig. 1(A). We present a zoomed-in image of the hex reconstruction in (B) and a zoomed-in image of the hex reconstruction next to a small Au(001)-(1 × 1) region in (C). Perpendicular to the hex rows, we observe the expected periodicity of 6 top layer atoms, on top of 5 atoms of the unreconstructed substrate. Such small unreconstructed regions are rare and easily "close-up", the hex rows experience lateral displacement in direction, perpendicular to the ribbons. Such displacements were reported before in electrochemical environment [21–23]. Because of that, the precise orientation of the hex ribbons with respect to the main ⟨011⟩ crystallographic direction cannot be deduced, but using the areas between lateral displacements suggests that any rotation of the hex layer is below 1°, consistent with previous reports [3,7,9]. Along the hex ribbons (Fig. 1(B)), the periodicity is about 17 atoms, which is close to the generally accepted $N \sim 20$ atoms. Additionally, as our measurements are performed at room temperature, there are always signatures of dynamic processes: even at the smallest scale in Fig. 1(B), clearly some areas feature atomic displacements, either due to the high mobility of the Au atoms, or because of interactions with the STM tip.

In summary, after sputtering and annealing, the surface is covered with the hex reconstruction, closely aligned to the main ⟨011⟩ crystallographic direction. Only rarely small Au(001)-(1 × 1) regions can be found which close in the order of tens of minutes (after a few STM images).

5. The decanethiol-modified surface landscape

After the sample is placed for 1 h in the decanethiol solution, the surface landscape is drastically altered. The hex reconstruction is lifted on a large scale. In Fig. 2 we show examples of the resulting landscapes. In (A) we show a large area that seems to be covered by a disordered decanethiol SAM. Upon zooming, sometimes the underlying lattice can be seen, corresponding to the unreconstructed Au(001)-(1 × 1) surface (see Fig. 2(B)). Such images could be rarely made, due to the streaky appearance which we assign to diffusing species which frequently interact with the tip (a disordered phase). Note that the majority of the diffusing entities must be chemisorbed, as described in the supplementary material, based on the fitting of the S2p region from X-ray photo-electron spectroscopy data.

In Fig. 2(C) and (D), we present another locally available landscape, in which monolayer-high Au islands have formed, and occasionally

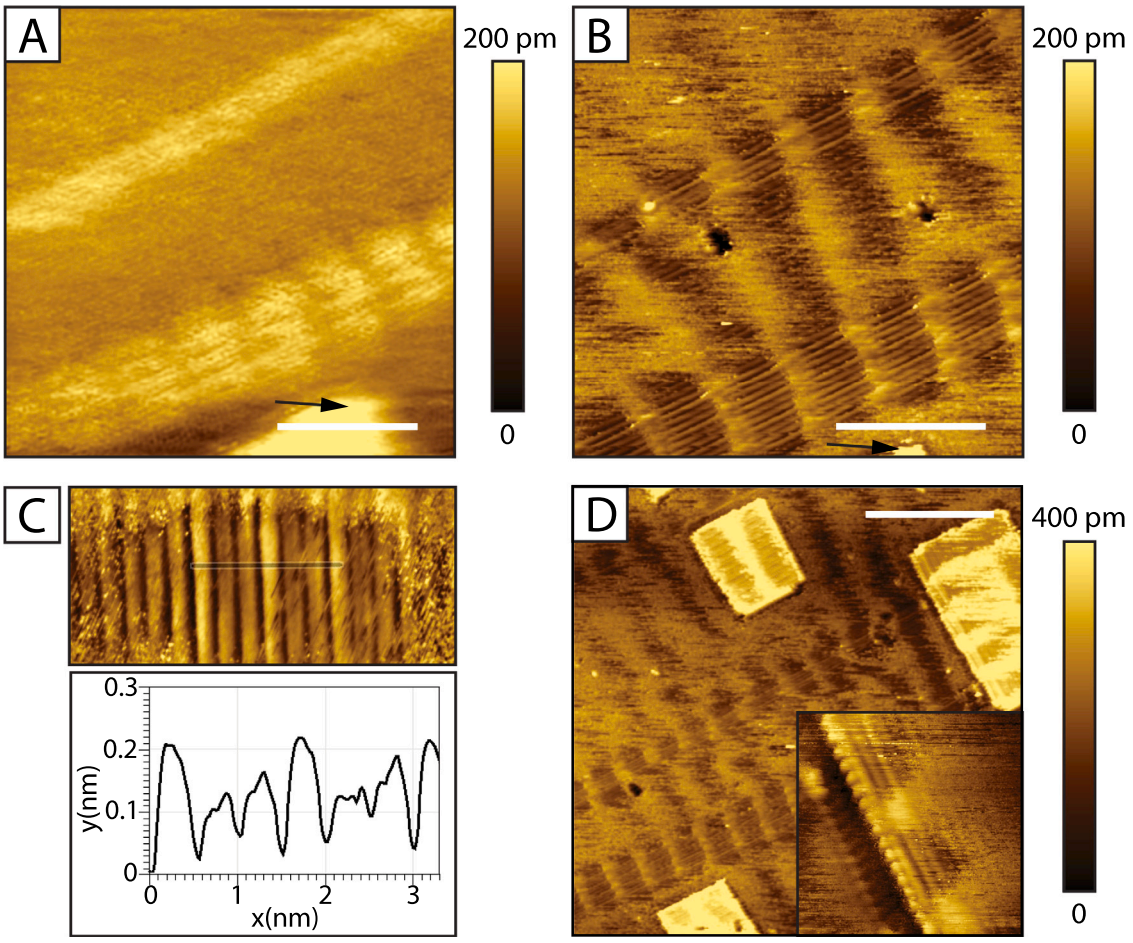

Fig. 3. STM data with enhanced contrast. (A) Image just before the enhanced contrast appeared. We observe 2 sets of hex stripes next to an island corner (indicated with an arrow). Set-points: 300 mV, 100 pA, scale bar: 10 nm. (B) Image just after the enhanced contrast appeared. We observe 2 sets of hex stripes next to an island corner (indicated with an arrow). Set-points: 300 mV, 100 pA, scale bar: 10 nm. (C) A zoomed-in STM image featuring the resulting pattern at the hex rows. A height profile is provided, demonstrating that the repeating pattern has a width which is very close to the width of the hex reconstruction, shown in Fig. 1 (D). (D) An STM image from a region nearby, also featuring Au islands, covered with analogous pattern as the rows shown in (C): partially hex-reconstructed islands. Scale bar: 20 nm. The inset is a 10 × 10 nm^2 STM image, close to the edge of an island, where also ordering is clearly visible.

a few hex stripes can be seen. The fuzzy appearance can be again assigned to a dynamic disordered phase. Nevertheless, upon increasing the tunneling current (moving closer to the surface), we can again resolve the landscape, shown as an inset in Fig. 2(D). The square pattern again corresponds to the unreconstructed Au(001)-(1 × 1) surface.

An alternative view of the surface is provided in Fig. 3, where the contrast in the STM images has changed, which we assign to potentially picking-up an object by the STM tip or tunneling to another available state (see Fig. 3 (A) and (B)). We observe a fuzzy appearance at the surface, excluding the areas of a few hex rows. Note that the periodicity of the hex ribbons is only partially resolved, but the width of the repeating pattern corresponds closely to the expected width of the hex reconstruction, as shown in (C). From Fig. 3(D) also becomes clear that the nearby islands are covered with an analogous pattern, suggesting that the islands are also already partially reconstructed. Finally, in the inset in (D) we observe an island edge, which is clearly decorated with an ordered pattern. Because the reason for the enhanced contrast cannot be unambiguously determined, the nature of the pattern cannot be identified, but it is important to note that this pattern does not change in time. Therefore, at some places on the surface, the growth/decay of Au-islands and step-edges has already taken place.

Considering the local landscapes that we have shown, the Au islands do not amount to 25% of the total surface. However, to obtain exact statistics is beyond the scope of this study. If the fuzzy areas that we measure contain Au-adatoms and Au-adatom-molecule complexes, then we would expect to observe at least sometimes growing Au islands or hex reconstruction areas. We note that such a place was discovered also as a locally available landscape on the sample (Fig. 4). However, the growth still did not proceed until total coverage with the hex phase. Some of the hex stripes grow at the expense of already present Au islands, while the area in between islands and hex rows remains less nicely resolved. This process resembles the already reported hex phase growth observed in electrochemical environment [17,23], and may also be enabled by the desorption of thiol molecules which is known to take place in UHV conditions [56]. The effect of the electric field of the STM tip may be responsible for the onset of the growth. The lifting of the hex reconstruction in UHV conditions was reported earlier [57]. Although we do not use a high voltage set-point, we cannot exclude the possibility that not only the lifting but onsetting the hex growth in UHV is possible due to the local field of the STM tip. Nevertheless, because such a region was observed only once and very locally, we are inclined to believe that most of the remaining adatoms released during the lifting of the hex phase are still obstructed by molecules.

In summary, we have examined a few available surface structures on the decanethiol-modified Au(001) surface in the low coverage regime. In all of these locations, a disordered phase on top of unreconstructed gold was observed, coexisting with partially reconstructed Au islands and occasionally a few hex stripes. We assign the fuzzy appearance of the disordered phase to diffusing species. If the molecular coverage is high enough, we must observe the formation of ordered decanethiol

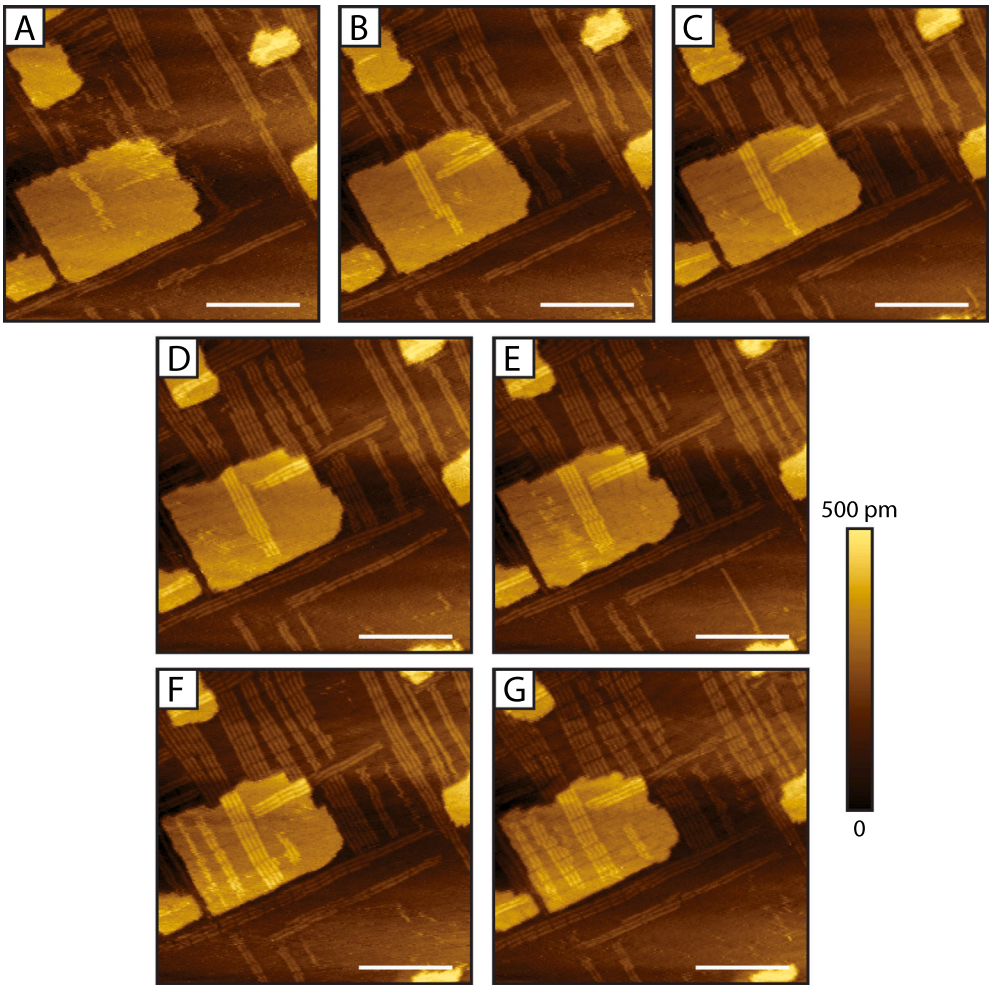

Fig. 4. (A)–(G) Sequence of 100 × 100 nm^2 STM images from a local area where the hex reconstruction experiences changes and growth in time. Set-points: 300 mV, 100 pA, scale bars: 30 nm. Each image is recorded in 6 min.

phases, while if the number of molecules is too low, then the surface must be slowly reconstructing again, as then the Au-adatoms can re-unite with the hex stripes and the islands. However, this was generally not observed: the landmarks in Figs. 2 and 3 are unaffected for hours, while the growth presented in Fig. 4 is an isolated local phenomenon. That is why, we are inclined to believe that the molecules on the surface participate in complexes, together with Au-adatoms. Further support for the higher dynamics in the disordered areas is provided in the next section.

6. Surface dynamics

To further support our observations from the previous section, we have performed $I(t)$ spectroscopy. We have previously used this powerful technique to study the dynamics of molecules and Ge dimers [50, 58–61]. In the current case this is an unambiguous method of indicating if the fuzzy areas presented so far indeed are more dynamic.

A grid measurement (Fig. 5(A)) was performed by disabling the feedback loop at each of the spectroscopic locations and recording an $I(t)$ trace for about 4 s. We selected an area where a hex stripe is visible, next to the typical disordered region.

Combining all the $I(t)$ traces, we have obtained a spatial heat map, i.e. a map of the dynamic activity, see Fig. 5(B). Based on the local mean for each $I(t)$ trace, we detect a switching phenomenon if the current difference between any two levels corresponds to at least 10% (10 pA) of the current set-point that we start with (100 pA). Additionally, the switch was counted as valid if the current levels participating in it are of given minimum length in time (about 60 ms), in order to avoid counting switches when the data is simply experiencing a sudden spike.

Because the grid is not as dense as the topographic image, we cannot resolve all the areas with great precision. However, the heat map in (B) directly correlates to the topography in (A). There is more variation in the current over time in the areas next to the hex stripes. This is consistent with the discussion presented in the previous section: at the non-reconstructed areas dynamic phenomena, probably due to the diffusion of molecules and adatoms or molecule-adatom complexes, take place.

From the residence times distribution in Fig. 5(C) we observe a linear dependence which indicates that the detected switching is stochastic. Moreover, from the slope of the curve ($\nu = 2.6$ Hz) we obtain that there are on average a bit less than 3 events per second, which take place between the tip and the surface. If we use that $\nu = \nu_0 e^{-E_d/kT}$, then we can obtain an upper limit for the diffusion barrier E_d. If we use ν_0 to be in the order of 10^{13} Hz, we obtain $E_d \sim 0.7$ eV at room temperature. However, the attempt frequency that we use here is typical for atoms. For molecules, the attempt frequency ν_0 can easily go down a few orders of magnitude, which considerably lowers the upper limit of the diffusion barrier relevant in order to observe the switching phenomena as reported here. Moreover, if we deal with more than one type of diffusing species, the interpretation of the data becomes a challenge.

That is why, in order to interpret further the contrast in dynamic behavior as presented in Figs. 5 and 3, we decided to perform DFT calculations of the activation barriers for diffusion for different decanethiol configurations, and then compare these for the reconstructed portion of the surface and the unreconstructed Au(001) surface.

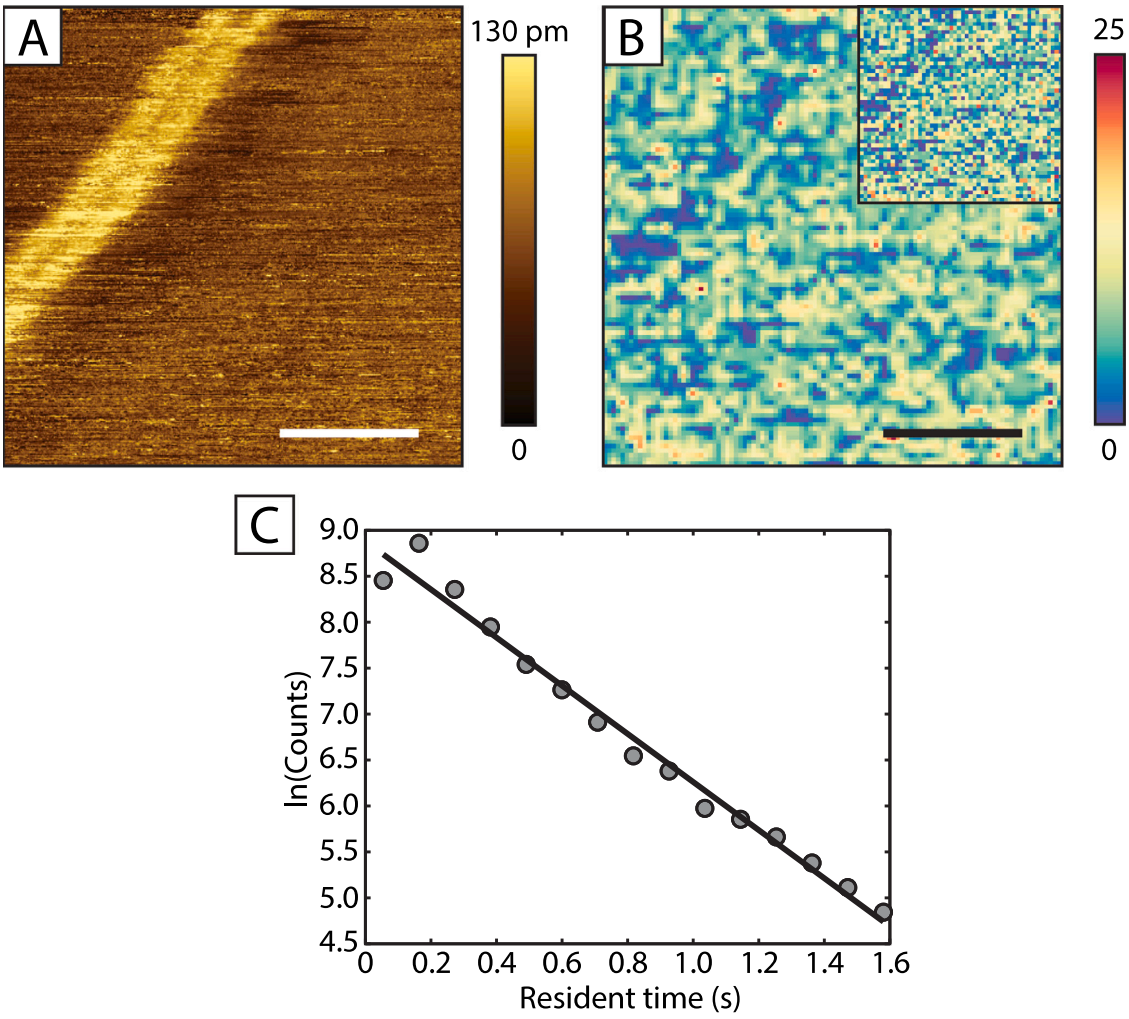

Fig. 5. (A) $I(t)$ grid (topography), set-points: 300 mV, 100 pA, scale bars in (A) and (B) correspond to 5 nm. Spectroscopy locations are set at each Au lattice spacing, about 0.3 nm apart. (B) $I(t)$ heatmap of the detected switches. We show interpolated data for clarity. In the inset, the original data is shown. (C) Distribution of residence times. The linear fit corresponds to the formula $-2.62x + 8.88$.

7. DFT results

To explain the dynamics on the surface we performed DFT calculations of the diffusion barriers for a few configurations. Based on the findings in the previous sections, we assume that we do not deal simply with the diffusion of Au-adatoms, as the surface would then slowly reconstruct at all locations on the sample. Therefore, in all of the configurations that we considered, a decanethiol molecule participates.

First, we found possible adsorption sites for the bare decanethiol molecule, then the Au–SR complex (the gold–decanethiol complex), and finally the RS–Au–SR complex (a gold atom with two decanethiols). All possible adsorption sites (upper, bridge, and hollow) on the unreconstructed surface were tested. It was found that the bridge sites are the most stable adsorption sites for the decanethiol molecule on Au(001), where the S atom binds to two neighboring surface gold atoms (the bridging motif). Similar behavior was found for methylthiolate on Au(100) [40]. The activation barriers for diffusion from one bridge site to another one for this system is 0.409 eV (see Fig. 6(A)).

Next, we investigated the diffusion of the Au–SR complex on the unreconstructed surface. The most stable structure was found when the Au-adatom is positioned in a hollow site. Note that the S atom is located next to one of the four gold surface atoms. As in the previous case, a S atom binds with two neighboring gold atoms. However, in this case, the activation barrier for diffusion is one and a half times smaller and equal to 0.285 eV (see Fig. 6(B)). The decrease in the value of the activation barrier of the Au-SR complex is probably due to the weaker interaction of the S atom with the gold atoms of the surface.

The more complex system (RS–Au–SR complex) was also investigated. Fig. 6(C) shows two optimized configurations for the RS–Au–SR complex. The most stable configuration (on the left panel in Fig. 6(C)) has the Au-adatom at the bridge site and the decanethiols are located diagonally across two neighboring opposite bridge positions. The second configuration (on the right panel) has the Au-adatom at the hollow site and decanethiols lay diagonally across one Au square unit cell. The activation barriers for diffusion from one configuration to another and back are 0.308 eV and 0.117 eV, respectively. Therefore, a comparison of the values of all activation barriers shows that the Au–SR complex is the most mobile on the surface than the other presented configurations. Note that the value of 0.285 eV is very close to the diffusion barrier of ~0.3 eV obtained in the study of Kim et al. for a bare Au-adatom on the unreconstructed Au(001) surface [62].

Finally, we aim to explain the contrast observed in the heat map in Fig. 5(B), or the generally more fuzzy appearance at the unreconstructed areas in all the data. We selected the most mobile Au–SR complex and investigated its diffusion on top of the hex reconstruction. In Fig. 6(D) we present the results for diffusion along the [011] direction, parallel to the hex row. Note that the hex reconstruction features quite a large unit cell which is a challenge to model. That is why, we present a simplified picture, based on Figure 1 from the

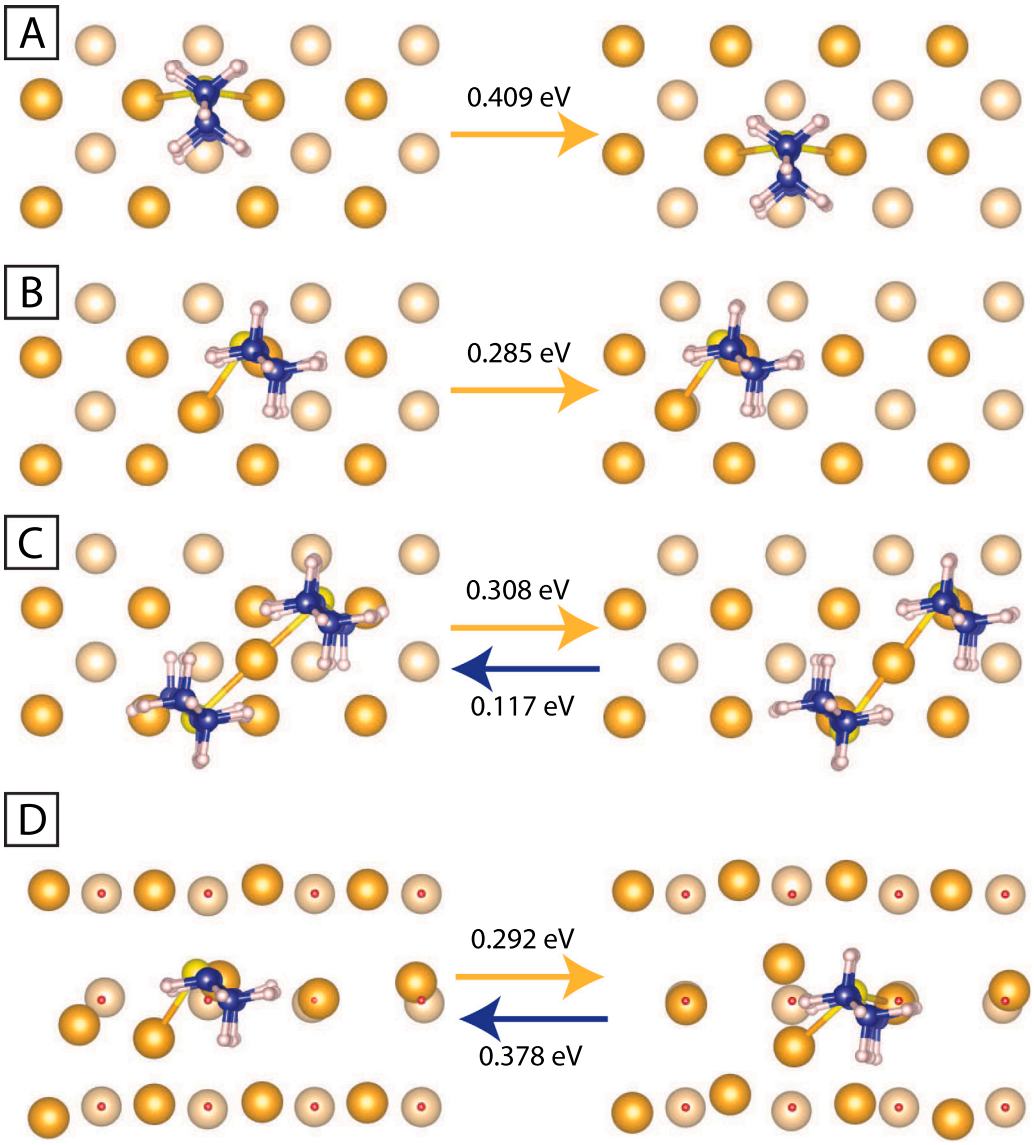

Fig. 6. Values of activation barriers for diffusion and atomic model of the adsorption configuration on Au(001)-(1 × 1) for decanethiol (A), decanethiol with a gold adatom (B), and a gold adatom with two decanethiols (C). Color code: Au (bottom) = light gold, Au (top) = dark gold, S = yellow, C = blue, H = white. (D) Activation barrier for diffusion and atomic model for adsorption in the case of the Au(001)-hex surface and decanethiol with a gold adatom. Note that the molecule diffusion leads to distortions in the Au layers. With red dots the unperturbed locations for the unreconstructed square lattice are given.

study of Hammer et al. [3]. We have modeled only a ridge area (labeled with "R" in the source). We have also assumed a commensurate structure, without mismatch between the top hexagonal layer and the second square layer of the Au surface. The obtained diffusion barriers for the presented configuration are higher compared to the barriers obtained for this complex on the unreconstructed surface. Therefore, the presence of complexes on the surface is not in contradiction with the contrast that we obtain in our data. Even for the configuration of lowest diffusion barrier on the unreconstructed surface, diffusion will be less likely on top of the hex portion of the surface. Note that the diffusion of the molecule on top of the surface in (D) leads to distortion of the whole structure as well (we have marked with red circles the location of the unperturbed unreconstructed surface). This is still in agreement with our data: the presence of too many molecules should then lead to the total lifting of the hex reconstruction and the formation of ordered phases. This is, however, not yet the case everywhere on the surface. Also, as for the unreconstructed surface, the obtained here diffusion barriers for the hex surface are also comparable to the self-diffusion barrier for an Au adatom. Trembulowicz et al. have obtained in an STM study a 0.32 eV barrier for the one dimensional diffusion along the hex rows [63].

8. Discussion

The fuzzy appearance in the STM images presented in this paper can be assigned to diffusing species: Au adatoms or decanethiol molecules. At this stage, Au-adatom-molecule complexes cannot be excluded. While these species diffuse quite fast, judging by the lack of ordering, the coverage is probably too low in order to form ordered decanethiol phases. The disordered regions are also confirmed to be more dynamic based on $I(t)$ spectroscopy data.

It can be speculated that some of the Au-adatoms released during the lifting of the hex reconstruction have been already ejected back to the surface: partially reconstructed Au islands are present, as well as the occasional few hex rows. However, the remaining Au-adatoms are still in the phase of diffusion on top of the surface, probably participating in molecular complexes. Only very locally the growth of the hex reconstruction was observed.

Exactly after the lifting of the hex reconstruction, we are provided with an adatom coverage of $\theta \sim 0.25$. In the case of lifting the herringbone reconstruction, the coverage is only about $\theta \sim 0.04$. To form enough staples, established as the building blocks of thiols on Au(111), additional Au atoms are picked from the terraces (and step-edges), which explains the presence of vacancy pits. As the Au(001) surface provides higher adatom coverage, it may not be necessary to create additional vacancy pits in the substrate terraces.

The highest coverage reported for alkanethiol phases on Au(001) corresponds to the so-called α phase [27,28,30,31]. The highest coverage reported for this phase is $\theta = 0.44$ ML [30,31]. Assuming that this phase coexists with other ordered phases, such as the β phase ($\theta \sim 0.33$), it becomes clear that the adatoms available upon lifting of the hex reconstruction would not be quite enough to be the building blocks of these phases. Even if we assume that two thiol molecules bind to the same Au-adatom, then the surface must remain mostly free of Au islands, while such are, however, frequently observed for thiol SAMs on Au(001). Additionally, some phases that we mentioned are reported to grow in regions where the hex reconstruction is not fully lifted. Therefore, assuming the staple as a building block of decanethiol phases on Au(001) is a challenging view. However, when we take into account that adatoms can be supplied by pre-existing step-edges or incorporated locally into new Au-adatom-island reservoirs, suddenly the constraints regarding the formation of the complexes are loosened. Of course, when the coverage of decanethiol molecules is high enough, it would be crucial how the potentially present Au-molecule complexes interact with each other. Considerable re-arrangements may still take place, which does not in particular negate the presence of molecule-adatom complexes as transport units.

Because Au(001) is a more open surface compared to Au(111), it is likely to expect that in the bridging motif, preferred on Au(001), the S–Au bonds are stronger and thiols are more strongly bound [40]. The higher stability of thiols on Au(001) w.r.t. SAMs on Au(111) has been already confirmed [64]. It is, therefore, not likely to have molecules on the Au(001) surface which participate in an ongoing diffusion process. Our results are in agreement with these previous reports: the diffusion barrier for bare decanethiol molecules is the highest among the configurations that we have considered. At the same time, we took a step further and considered two types of Au-molecule complexes. Even the complicated 2-molecule complex, shown in Fig. 6(C) is more mobile than a bare decanethiol molecule. These results are also in agreement with studies for thiols on Au(111): it was shown that the staple has lower diffusion barrier than the bare thiol radical [65]. The diffusion barriers that we obtain are also higher than the barriers for Au(111) [50]. Our results can also explain the contrast in dynamic behavior in the STM data presented. The Au–SR complex, which apart from bare Au-adatoms, based on the obtained diffusion barriers, is the most likely diffusing complex on the unreconstructed Au(001) surface, features a lower diffusion barrier for the unreconstructed surface as compared to the reconstructed portions of the surface.

9. Conclusion

We presented a study of decanethiol SAM on Au(001) in the lowest coverage regime for which no ordered phases form. Based on the observed dynamics in the STM data, we suggest that molecule-Au-adatom complexes continuously diffuse on top of the surface, but the coverage is too low in order to form nucleation centers and onset the growth of phases. Based on DFT results, we showed that the most likely diffusing moieties are Au–SR complexes in which a single decanethiol molecule binds to a Au-adatom. Even if two molecules bind to a single Au-adatom, the diffusion barrier remains lower compared to a bare thiol.

Considering the theoretically available Au-adatoms after the lifting of the hex reconstruction, it is clear that at higher coverage there would be hardly enough complexes to build the generally reported thiol phases if we consider that each molecule (or each two molecules) are bind to a Au-adatom. However, adatoms can be also supplied from step edges, which is hard to trace when the growth is not observed in real time. How ordered decanethiol phases exactly form is beyond the scope of our research. Such information will be accessible by depositing the thiol molecules *in-situ* in UHV conditions, preferably both on Au(001)-hex and Au(001)-(1 × 1) at various coverage limits. This comparison will be crucial while observing the growth in real time. Nevertheless, our results suggest the universal conjecture that irrespective of the surface orientation, molecule-Au-adatom complexes may remain the main diffusing units on the gold surfaces. We speculate that the lack of Au-vacancy pits should no longer be considered a sufficient proof for the lack of complexes formation.

The complexes should be also more frequently addressed in computational studies. Even if it is not likely to have all phases build up by complexes, exploring the interactions between neighboring entities on the surface is still crucial for the understanding of how phases may form and stabilize. The low coverage regime is especially interesting, as the supplied atoms by the lifting of the hex reconstruction are still enough to form complexes with most of the molecules.

CRediT authorship contribution statement

Martina Tsvetanova: Conceptualisation, Methodology, Validation, Formal analysis, Investigation, Writing – original draft, Writing – review & editing, Visualisation. **Alexey G. Syromyatnikov:** Methodology, Software, Formal analysis, Investigation, Writing – original draft, Visualisation. **Harold J.W. Zandvliet:** Conceptualisation, Writing – review & editing. **Andrey L. Klavsyuk:** Methodology, Software, Formal analysis, Investigation, Writing – original draft, Visualisation. **Kai Sotthewes:** Conceptualisation, Methodology, Formal analysis, Writing – review & editing.

Declaration of competing interest

The authors declare that they have no known competing financial interests or personal relationships that could have appeared to influence the work reported in this paper.

Acknowledgments

The authors would like to thank Dr. H. Wu for the fruitful discussions. M. Tsvetanova, K. Sotthewes, and H. J. W. Zandvliet acknowledge the Nederlandse organisatie voor Wetenschappelijk Onderzoek (NWO) for the provided financial support. The density functional theory calculations were performed using the equipment of the shared research facilities of HPC computing resources at the Lomonosov Moscow State University. Calculations of this study was financially supported by the Russian Science Foundation (project No. 21-72-20034). The authors also acknowledge the support of dr. Y. Bu from the MESA+ Institute for Nanotechnology Nanolab, Enschede, the Netherlands, for performing the XPS measurement presented in the supplementary information of this paper.

Appendix A. Supplementary data

Supplementary material related to this article can be found online at https://doi.org/10.1016/j.apsusc.2022.153364.

References

[1] D.G. Fedak, N.A. Gjostein, On the anomalous surface structures of gold, Surf. Sci. 8 (1967) 77–97, http://dx.doi.org/10.1016/0039-6028(67)90074-X.

[2] D.M. Zehner, B.R. Appleton, T.S. Noggle, J.W. Miller, J.H. Barrett, L.H. Jenkins, O.E. Schow, Characterization of reordered (001) Au surfaces by positive-ion-channeling spectroscopy, LEED, and AES, J. Vac. Sci. Technol. 12 (1) (1975) 454, http://dx.doi.org/10.1116/1.568600.

[3] R. Hammer, A. Sander, S. Förster, M. Kiel, K. Meinel, W. Widdra, Surface reconstruction of Au(001): High-resolution real-space and reciprocal-space inspection, Phys. Rev. B 90 (3) (2014) 035446, http://dx.doi.org/10.1103/PhysRevB.90.035446.

[4] P. Havu, V. Blum, V. Havu, P. Rinke, M. Scheffler, Large-scale surface reconstruction energetics of Pt(100) and Au(100) by all-electron density functional theory, Phys. Rev. B 82 (16) (2010) 161418, http://dx.doi.org/10.1103/PhysRevB.82.161418.

[5] E. Bauer, A.K. Green, K.M. Kunz, On the epitaxial growth of single-crystal metal films free of impurities, Appl. Phys. Lett. 8 (10) (1966) 248–249, http://dx.doi.org/10.1063/1.1754422.

[6] P.W. Palmberg, T.N. Rhodin, Surface structure of clean au (100) and Ag (100) surfaces, Phys. Rev. 161 (3) (1967) 586–588, http://dx.doi.org/10.1103/PhysRev.161.586.

[7] H. Melle, E. Menzel, Superstructures on spherical gold crystals, Z. Naturforschung A 33 (3) (1978) 282–289, http://dx.doi.org/10.1515/zna-1978-0305.

[8] M.A. Van Hove, R.J. Koestner, P.C. Stair, J.P. Bibérian, L.L. Kesmodel, I. Bartoš, G.A. Somorjai, The surface reconstructions of the (100) crystal faces of iridium, platinum and gold. I. Experimental observations and possible structural models, Surf. Sci. 103 (1) (1981) 189–217, http://dx.doi.org/10.1016/0039-6028(81)90107-2.

[9] K. Yamazaki, K. Takayanagi, Y. Tanishiro, K. Yagi, Transmission electron microscope study of the reconstructed Au(001) surface, Surf. Sci. 199 (3) (1988) 595–608, http://dx.doi.org/10.1016/0039-6028(88)90924-7.

[10] D. Gibbs, B.M. Ocko, D.M. Zehner, S.G. Mochrie, Structure and phases of the Au(001) surface: In-plane structure, Phys. Rev. B 42 (12) (1990) 7330–7344, http://dx.doi.org/10.1103/PhysRevB.42.7330.

[11] O.K. Binnig, H. Rohrer, C. Gerber, E. Stoll, Real-space observation of the reconstruction of Au(100), Surf. Sci. 144 (2–3) (1984) 321–335, http://dx.doi.org/10.1016/0039-6028(84)90104-3.

[12] O. Rodríguez de la Fuente, M.A. González, J.M. Rojo, Ion bombardment of reconstructed metal surfaces: From two-dimensional dislocation dipoles to vacancy pits, Phys. Rev. B 63 (8) (2001) 085420, http://dx.doi.org/10.1103/PhysRevB.63.085420.

[13] V. Navarro, O. Rodríguez De La Fuente, A. Mascaraque, J.M. Rojo, Plastic properties of gold surfaces nanopatterned by ion beam sputtering, J. Phys.: Condens. Matter 21 (22) (2009) 224023, http://dx.doi.org/10.1088/0953-8984/21/22/224023.

[14] A. Trembulowicz, B. Pieczyrak, L. Jurczyszyn, G. Antczak, Coexistence of nanowire-like hex and (1x1) phases in the topmost layer of Au(100) surface, Nanotechnology 30 (4) (2019) 045704, http://dx.doi.org/10.1088/1361-6528/aaed7f.

[15] F. Ercolessi, E. Tosatti, M. Parrinello, Au (100) surface reconstruction, Phys. Rev. Lett. 57 (6) (1986) 719–722, http://dx.doi.org/10.1103/PhysRevLett.57.719.

[16] B. Pieczyrak, A. Trembulowicz, G. Antczak, L. Jurczyszyn, Nature of monovacancies on quasi-hexagonal structure of reconstructed Au(100) surface, Appl. Surf. Sci. 407 (2017) 345–352, http://dx.doi.org/10.1016/j.apsusc.2017.02.089.

[17] O.M. Magnussen, J. Hotlos, R.J. Behm, N. Batina, D.M. Kolb, An in-situ scanning tunneling microscopy study of electrochemically induced "hex" ↔ (1×1) transitions on Au(100) electrodes, Surf. Sci. 296 (3) (1993) 310–332, http://dx.doi.org/10.1016/0039-6028(93)90027-H.

[18] X. Gao, A. Hamelin, M.J. Weaver, Potential-dependent reconstruction at ordered Au(100)-aqueous interfaces as probed by atomic-resolution scanning tunneling microscopy, Phys. Rev. Lett. 67 (5) (1991) 618–621, http://dx.doi.org/10.1103/PhysRevLett.67.618.

[19] X. Gao, M.J. Weaver, Electrode potential-induced reconstruction of Au(100): Effect of chemisorption on nanoscale dynamics as probed by in-situ scanning tunneling microscopy, J. Phys. Chem. 97 (34) (1993) 8685–8689, http://dx.doi.org/10.1021/j100136a004.

[20] N. Batina, A.S. Dakkouri, D.M. Kolb, The surface structure of flame-annealed Au(100) in aqueous solution: An STM study, J. Electroanal. Soc. 370 (1) (1994) 87–94, http://dx.doi.org/10.1016/0022-0728(93)03212-8.

[21] M. Labayen, C. Ramirez, W. Schattke, O.M. Magnussen, Quasi-collective motion of nanoscale metal strings in metal surfaces, Nature Mater. 2 (12) (2003) 783–787, http://dx.doi.org/10.1038/nmat1011.

[22] M. Labayen, O.M. Magnussen, In-situ video-STM studies of the quasi-collective motion of nanoscale metal strings in Au(100) electrode surfaces, Microsc. Microanal. 9 (2003) 904–905, http://dx.doi.org/10.1017/s1431927603444528.

[23] M. Labayen, O.M. Magnussen, In situ video-STM study of the potential-induced (1×1) → "hex" transition on Au(100) electrode surfaces in Cl^- containing solution, Surf. Sci. 573 (1) (2004) 128–139, http://dx.doi.org/10.1016/j.susc.2004.05.143.

[24] S. Yoshimoto, Y.-G. Kim, K. Sato, J. Inukai, K. Itaya, Potential-induced phase transition of low-index Au single crystal surfaces in propylene carbonate solution, Phys. Chem. Chem. Phys. 14 (7) (2012) 2286–2291, http://dx.doi.org/10.1039/c2cp23171a.

[25] Y.J. Feng, K.P. Bohnen, C.T. Chan, First-principles studies of Au(100)-hex reconstruction in an electrochemical environment, Phys. Rev. B 72 (12) (2005) 125401, http://dx.doi.org/10.1103/PhysRevB.72.125401.

[26] K.P. Bohnen, D.M. Kolb, Charge- versus adsorbate-induced lifting of the Au(100)-(hex) reconstruction in an electrochemical environment, Surf. Sci. 407 (1–3) (1998) L629–L632, http://dx.doi.org/10.1016/S0039-6028(98)00232-5.

[27] M. Schweizer, H. Hagenström, D.M. Kolb, Potential-induced structure transitions in self-assembled monolayers: ethanethiol on Au (100), Surf. Sci. 490 (3) (2001) L627–L636, http://dx.doi.org/10.1016/S0039-6028(01)01377-2.

[28] M. Schweizer, M. Manolova, D.M. Kolb, Potential-induced structure transitions in self-assembled monolayers: II. Propanethiol on Au(100), Surf. Sci. 602 (21) (2008) 3303–3307, http://dx.doi.org/10.1016/j.susc.2008.09.009.

[29] F. Loglio, M. Schweizer, D.M. Kolb, In situ characterization of self-assembled butanethiol monolayers on Au(100) electrodes, Langmuir 19 (3) (2003) 830–834, http://dx.doi.org/10.1021/la026493y.

[30] D. Grumelli, L.J. Cristina, F.L. Maza, P. Carro, J. Ferrón, K. Kern, R.C. Salvarezza, Thiol adsorption on the Au(100)-hex and Au(100)-(1×1) surfaces, J. Phys. Chem. C 119 (25) (2015) 14248–14254, http://dx.doi.org/10.1021/acs.jpcc.5b03931.

[31] D. Grumelli, F.L. Maza, K. Kern, R.C. Salvarezza, P. Carro, Surface structure and chemistry of alkanethiols on Au(100)-(1×1) substrates, J. Phys. Chem. C 120 (1) (2016) 291–296, http://dx.doi.org/10.1021/acs.jpcc.5b09459.

[32] R. Yamada, K. Uosaki, Structural investigation of the self-assembled monolayer of decanethiol on the reconstructed and (1×1)-Au(100) surfaces by scanning tunneling microscopy, Langmuir 17 (14) (2001) 4148–4150, http://dx.doi.org/10.1021/la010470m.

[33] G.E. Poirier, Butanethiol self-assembly on Au(001): The 1x4 Au missing row, c(2x8) molecular lattice, J. Vac. Sci. Technol. B 14 (2) (1996) 1453–1460, http://dx.doi.org/10.1116/1.589118.

[34] G.E. Poirier, Coverage-dependent phases and phase stability of decanethiol on Au(111), Langmuir 15 (4) (1999) 1167–1175, http://dx.doi.org/10.1021/la981374x.

[35] G.E. Poirier, W.P. Fitts, J.M. White, Two-dimensional phase diagram of decanethiol on Au(111), Langmuir 17 (4) (2001) 1176–1183, http://dx.doi.org/10.1021/la0012788.

[36] G.E. Poirier, Mechanism of formation of Au vacancy islands in alkanethiol monolayers on Au(111), Langmuir 13 (7) (1997) 2019–2026, http://dx.doi.org/10.1021/la960777z.

[37] P. Maksymovych, O. Voznyy, D.B. Dougherty, D.C. Sorescu, J.T. Yates, Gold adatom as a key structural component in self-assembled monolayers of organosulfur molecules on Au(111), Prog. Surf. Sci. 85 (5–8) (2010) 206–240, http://dx.doi.org/10.1016/j.progsurf.2010.05.001.

[38] V. Rojas-Cervellera, E. Giralt, C. Rovira, Staple motifs, initial steps in the formation of thiolate-protected gold nanoparticles: How do they form? Inorg. Chem. 51 (21) (2012) 11422–11429, http://dx.doi.org/10.1021/ic301079k.

[39] J. Gao, F. Li, G. Zhu, Z. Yang, H. Lu, H. Lin, Q. Li, Y. Li, M. Pan, Q. Guo, Spontaneous breaking and remaking of the RS–Au–SR staple in self-assembled ethylthiolate/Au(111) interface, J. Phys. Chem. C 122 (34) (2018) 19473–19480, http://dx.doi.org/10.1021/acs.jpcc.8b04157.

[40] G. Hu, R. Jin, D.E. Jiang, Beyond the staple motif: a new order at the thiolate-gold interface, Nanoscale 8 (48) (2016) 20103–20110, http://dx.doi.org/10.1039/c6nr07709a.

[41] P. Carro, K. Müller, F.L. Maza, C. Vericat, U. Starke, K. Kern, R.C. Salvarezza, D. Grumelli, 6-mercaptopurine self-assembled monolayers on gold (001)-hex: revealing the fate of gold adatoms, J. Phys. Chem. C 121 (16) (2017) 8938–8943, http://dx.doi.org/10.1021/acs.jpcc.7b02732.

[42] E. Pensa, P. Carro, A.A. Rubert, G. Benítez, C. Vericat, R.C. Salvarezza, Thiol with an unusual adsorption-desorption behavior: 6-Mercaptopurine on Au(111), Langmuir 26 (22) (2010) 17068–17074, http://dx.doi.org/10.1021/la102441b.

[43] F. Lobo Maza, D. Grumelli, P. Carro, C. Vericat, K. Kern, R.C. Salvarezza, The role of the crystalline face in the ordering of 6-mercaptopurine self-assembled monolayers on gold, Nanoscale 8 (2016) 17231–17240, http://dx.doi.org/10.1039/C6NR06148F.

[44] F.L. Maza, P. Carro, C. Vericat, K. Kern, R.C. Salvarezza, D. Grumelli, Role of gold adatoms in the adsorption of sulfide species on the gold(001)-hex surface, J. Phys. Chem. C 122 (4) (2018) 2207–2214, http://dx.doi.org/10.1021/acs.jpcc.7b11059.

[45] G. Kresse, J. Hafner, Ab initio molecular dynamics for open-shell transition metals, Phys. Rev. B 48 (17) (1993) 13115–13118, http://dx.doi.org/10.1103/PhysRevB.48.13115.

[46] G. Kresse, J. Furthmüller, Efficient iterative schemes for ab initio total-energy calculations using a plane-wave basis set, Phys. Rev. B 54 (16) (1996) 11169–11186, http://dx.doi.org/10.1103/PhysRevB.54.11169.

[47] P.E. Blöchl, Projector augmented-wave method, Phys. Rev. B 50 (24) (1994) 17953–17979, http://dx.doi.org/10.1103/PhysRevB.50.17953.

[48] G. Kresse, D. Joubert, From ultrasoft pseudopotentials to the projector augmented-wave method, Phys. Rev. B 59 (3) (1999) 1758–1775, http://dx.doi.org/10.1103/PhysRevB.59.1758.

[49] J.P. Perdew, K. Burke, M. Ernzerhof, Generalized gradient approximation made simple, Phys. Rev. Lett. 77 (18) (1996) 3865–3868, http://dx.doi.org/10.1103/PhysRevLett.77.3865.
[50] O. Kap, N. Kabanov, M. Tsvetanova, C. Varlikli, A.L. Klavsyuk, H.J.W. Zandvliet, K. Sotthewes, Structural stability of physisorbed air-oxidized decanethiols on Au(111), J. Phys. Chem. C 124 (22) (2020) 11977–11984, http://dx.doi.org/10.1021/acs.jpcc.0c02806.
[51] H.J. Monkhorst, J.D. Pack, Special points for Brillouin-zone integrations, Phys. Rev. B 13 (12) (1976) 5188–5192, http://dx.doi.org/10.1103/PhysRevB.13.5188.
[52] S.N. Steinmann, C. Corminboeuf, Comprehensive benchmarking of a density-dependent dispersion correction, J. Chem. Theory Comput. 7 (11) (2011) 3567–3577, http://dx.doi.org/10.1021/ct200602x.
[53] G. Henkelman, H. Jónsson, Improved tangent estimate in the nudged elastic band method for finding minimum energy paths and saddle points, J. Chem. Phys. 113 (22) (2000) 9978–9985, http://dx.doi.org/10.1063/1.1323224.
[54] G. Henkelman, B.P. Uberuaga, H. Jónsson, A climbing image nudged elastic band method for finding saddle points and minimum energy paths, J. Chem. Phys. 113 (22) (2000) 9901–9904, http://dx.doi.org/10.1063/1.1329672.
[55] K. Momma, F. Izumi, VESTA 3 for three-dimensional visualization of crystal, volumetric and morphology data, J. Appl. Crystallogr. 44 (6) (2011) 1272–1276, http://dx.doi.org/10.1107/S0021889811038970.
[56] L.J. Cristina, G. Ruano, R. Salvarezza, J. Ferrón, Thermal stability of self-assembled monolayers of n-Hexanethiol on Au(111)-(1x1) and Au(001)-(1x1), J. Phys. Chem. C 121 (50) (2017) 27894–27904, http://dx.doi.org/10.1021/acs.jpcc.7b05883.
[57] J. Buisset, H.P. Rust, E.K. Schweizer, L. Cramer, A.M. Bradshaw, Tip-induced lifting of the Au100 (hex)-phase reconstruction in a low temperature ultrahigh vacuum scanning tunneling microscope, J. Vac. Sci. Technol. B 14 (2) (1996) 1117–1120, http://dx.doi.org/10.1116/1.588411.
[58] H. Wu, K. Sotthewes, A. Kumar, G.J. Vancso, P.M. Schön, H.J.W. Zandvliet, Dynamics of decanethiol self-assembled monolayers on Au(111) studied by time-resolved scanning tunneling microscopy, Langmuir 29 (7) (2013) 2250–2257, http://dx.doi.org/10.1021/la304902y.
[59] K. Sotthewes, R. Heimbuch, H.J.W. Zandvliet, Dynamics of copper-phthalocyanine molecules on Au/Ge(001), J. Chem. Phys. 143 (13) (2015) 134303, http://dx.doi.org/10.1063/1.4932190.
[60] A. van Houselt, R. van Gastel, B. Poelsema, H.J.W. Zandvliet, Dynamics and energetics of Ge(001) dimers, Phys. Rev. Lett. 97 (26) (2006) 266104, http://dx.doi.org/10.1103/PhysRevLett.97.266104.
[61] A. Saedi, A. van Houselt, R. van Gastel, B. Poelsema, H.J.W. Zandvliet, Playing pinball with atoms, Nano Lett. 9 (5) (2009) 1733–1736, http://dx.doi.org/10.1021/nl8022884.
[62] S.Y. Kim, I.-H. Lee, S. Jun, Transition-pathway models of atomic diffusion on fcc metal surfaces. I. Flat surfaces, Phys. Rev. B 76 (2007) 245407, http://dx.doi.org/10.1103/physrevb.76.245407.
[63] A. Trembulowicz, G. Ehrlich, G. Antczak, Surface diffusion of gold on quasihexagonal-reconstructed Au(100), Phys. Rev. B 84 (24) (2011) 245445, http://dx.doi.org/10.1103/PhysRevB.84.245445.
[64] N. Arisnabarreta, G.D. Ruano, M. Lingenfelder, E.M. Patrito, F.P. Cometto, Comparative study of the adsorption of thiols and selenols on Au(111) and Au(100), Langmuir 33 (48) (2017) 13733–13739, http://dx.doi.org/10.1021/acs.langmuir.7b03038.
[65] F.P. Cometto, P. Paredes-Olivera, V.A. Macagno, E.M. Patrito, Density functional theory study of the adsorption of alkanethiols on Cu(111), Ag(111), and Au(111) in the low and high coverage regimes, J. Phys. Chem. B 109 (46) (2005) 21737–21748, http://dx.doi.org/10.1021/jp053273v.